

## Synthesis and Characterization of Three Homoleptic Alkoxides of Uranium: $[\text{Li}(\text{THF})_2][\text{U}^{\text{IV}}(\text{O}^t\text{Bu})_6]$ , $[\text{Li}(\text{Et}_2\text{O})][\text{U}^{\text{V}}(\text{O}^t\text{Bu})_6]$ , and $\text{U}^{\text{VI}}(\text{O}^t\text{Bu})_6$

Skye Fortier, Guang Wu, and Trevor W. Hayton\*

Department of Chemistry and Biochemistry, University of California Santa Barbara, Santa Barbara, California 93106

Received January 14, 2008

Addition of 6 equiv of  $\text{LiO}^t\text{Bu}$  to a THF/ $\text{Et}_2\text{O}$  solution of  $\text{UCl}_4$  at  $-25\text{ }^\circ\text{C}$  generates  $[\text{Li}(\text{THF})_2][\text{U}(\text{O}^t\text{Bu})_6]$  (**1**) in 61% yield. **1** is soluble in polar organic solvents and is stable for several days in THF. However, **1** slowly decomposes in benzene or hexanes, forming the dinuclear uranium(IV) species  $[\text{Li}(\text{THF})][\text{U}_2(\text{O}^t\text{Bu})_9]$  (**2**) as one of the decomposition products. Alternatively, **2** can be directly prepared in moderate yield by the addition of 4.5 equiv  $\text{LiO}^t\text{Bu}$  to  $\text{UCl}_4$  in hexanes/THF at room temperature. The decomposition of **1** has been studied by  $^1\text{H}$  and  $^7\text{Li}\{^1\text{H}\}$  NMR spectroscopies to elucidate the nature of this transformation. Oxidation of **1** occurs readily in the presence of 0.5 or 1 equiv of  $\text{I}_2$  to give  $[\text{Li}(\text{Et}_2\text{O})][\text{U}(\text{O}^t\text{Bu})_6]$  (**3**) and  $\text{U}(\text{O}^t\text{Bu})_6$  (**4**), respectively, in good yields. Alternately, **3** can be generated by comproportionation of **1** and **4**. **1**–**4** have been fully characterized, including analysis by X-ray crystallography. In the solid-state these complexes possess large  $\text{U}-\text{O}-\text{C}_q$  bond angles, suggestive of a significant  $\text{U}-\text{O} \pi$  interaction. In addition, we have studied the redox properties of **4** by cyclic voltammetry.

### Introduction

Studies of uranium in the 6+ oxidation state are generally confined to species containing the uranyl ion ( $\text{UO}_2^{2+}$ ),<sup>1</sup> and more recently, its bis(imido) analogues ( $\text{U}(\text{NR})_2^{2+}$ ).<sup>2,3</sup> Other than the oxo and imido functionalites found in these complexes, very few ligand sets are capable of stabilizing the 6+ oxidation state of uranium.<sup>4</sup> An exception to this is the alkoxide class of ligands, which can form stable  $\text{U}(\text{VI})$  complexes with the general formula  $\text{U}(\text{OR})_6$ .<sup>5</sup> The synthesis and preparation of uranium alkoxides was first explored during the Manhattan Project in the search for volatile uranium compounds necessary for efficient uranium isotope separation. During this era, the preparation of several uranium alkoxides, including  $\text{U}(\text{OEt})_4$ ,  $\text{U}(\text{OEt})_5$ ,  $\text{Na}[\text{U}(\text{OEt})_6]$ , and  $\text{U}(\text{OEt})_6$ , was undertaken and later

reported by Gilman.<sup>6–12</sup> The alkoxide chemistry of uranium was further expanded in subsequent investigations by Bradley and co-workers,<sup>13–18</sup> and they reported the isolation of  $\text{U}(\text{O}^i\text{Pr})_6$ ,  $\text{U}(\text{O}^t\text{Bu})_6$ , and  $\text{U}(\text{O}^n\text{Bu})_6$  during this period.<sup>15</sup>

\* To whom correspondence should be addressed. Email: hayton@chem.ucsb.edu.

- (1) Denning, R. G. *J. Phys. Chem. A* **2007**, *111*, 4125–4143.
- (2) Hayton, T. W.; Boncella, J. M.; Palmer, P. D.; Scott, B. L.; Batista, E. R.; Hay, P. J. *Science* **2005**, *310*, 1941–1943.
- (3) Hayton, T. W.; Boncella, J. M.; Scott, B. L.; Batista, E. R.; Hay, P. J. *J. Am. Chem. Soc.* **2006**, *128*, 10549–10559.
- (4) Katz, J. J.; Seaborg, G. T.; Morss, L. R. *The Chemistry of the Actinide Elements*. 2nd ed.; Chapman and Hall: New York, 1986; Vol. 1.
- (5) Van Der Sluys, W. G.; Sattelberger, A. P. *Chem. Rev.* **1990**, *90*, 1027–1040.

- (6) Gilman, H.; Jones, R. G.; Bindschadler, E.; Blume, D.; Karmas, G.; Nobis, J. F.; Thirtle, J. R.; Yale, H. L.; Yeoman, F. A. *J. Am. Chem. Soc.* **1956**, *78*, 2790–2792.
- (7) Gilman, H.; Jones, R. G.; Karmas, G., Jr. *J. Am. Chem. Soc.* **1956**, *78*, 4285–4286.
- (8) Gilman, H.; Jones, R. G.; Bindschadler, E.; Karmas, G.; Yeoman, F. A. *J. Am. Chem. Soc.* **1956**, *78*, 4287–4288.
- (9) Gilman, H.; Jones, R. G.; Bindschadler, E.; Karmas, G., Jr.; Thirtle, J. R.; Yeoman, F. A. *J. Am. Chem. Soc.* **1956**, *78*, 4289–4291.
- (10) Gilman, H.; Jones, R. G.; Bindschadler, E.; Blume, D.; Karmas, G., Jr.; Thirtle, J. R. *J. Am. Chem. Soc.* **1956**, *78*, 6027–6029.
- (11) Gilman, H.; Jones, R. G.; Bindschadler, E.; Blume, D.; Karmas, G., Jr.; Thirtle, J. R.; Yeoman, F. A. *J. Am. Chem. Soc.* **1956**, *78*, 6030–6032.
- (12) Gilman, H.; Jones, R. G.; Bindschadler, E., Jr.; Thirtle, J. R. *J. Am. Chem. Soc.* **1957**, *79*, 4921–4922.
- (13) Bradley, D. C.; Chakravarti, B. N.; Chatterjee, A. K. *J. Inorg. Nucl. Chem.* **1957**, *3*, 367–369.
- (14) Bradley, D. C.; Chatterjee, A. K. *J. Inorg. Nucl. Chem.* **1957**, *4*, 279–281.
- (15) Bradley, D. C.; Chatterjee, A. K.; Chatterjee, A. K. *J. Inorg. Nucl. Chem.* **1959**, *12*, 71–79.
- (16) Bradley, D. C.; Kapoor, R. N.; Smith, B. C. *J. Inorg. Nucl. Chem.* **1962**, *24*, 863–867.
- (17) Bradley, D. C.; Kapoor, R. N.; Smith, B. C. *J. Chem. Soc.* **1963**, 204–207.
- (18) Bradley, D. C.; Kapoor, R. N.; Smith, B. C. *J. Chem. Soc.* **1963**, 1023–1027.

However, the materials produced by Gilman and Bradley were only partially characterized by modern standards, and little structural information was obtained.

Twenty years later, volatile uranium alkoxides were revisited as possible candidates for laser-induced isotope separation.<sup>19–22</sup> These studies focused primarily on the uranium(VI) complex  $U(OCH_3)_6$  and its fluoride-substituted derivatives, that is,  $U(OCH_3)_x F_{6-x}$ ,<sup>20,21</sup> and included a thorough bonding analysis of  $U(OMe)_6$  by PES and theoretical calculations.<sup>22</sup> The homoleptic uranium(IV) methoxide,  $Li_2[U(OMe)_6]$ , was also reported during these investigations, but this insoluble material could not be fully characterized.<sup>21</sup>

Gilman also reported the isolation of  $U(O^tBu)_4$  from the reaction of  $HO^tBu$  with “ $U(NH_2)_4$ ”.<sup>7</sup> However, subsequent investigations have shown that the product that Gilman isolated was probably  $K[U_2(O^tBu)_9]$ .<sup>23–26</sup>  $K[U_2(O^tBu)_9]$  is unstable in solution above 5 °C and at higher temperatures spontaneously converts to the mixed-valent species  $U_2(O^tBu)_9$ .<sup>24</sup> In addition, Cotton and co-workers reported that solutions of  $K[U_2(O^tBu)_9]$  in hexanes slowly convert to the oxo-capped trinuclear complex,  $U_3(O)(O^tBu)_{10}$ , over the course of several weeks.<sup>23,27</sup> The formation of this complex is most likely due to exposure of  $K[U_2(O^tBu)_9]$  to adventitious water.<sup>25</sup> Finally,  $U_2(O^tBu)_8(HO^tBu)$ , which is probably isostructural with  $[U_2(O^tBu)_9]^-$ , has also been isolated.<sup>25</sup>

Our interest in  $U(OR)_6$  and the 6+ oxidation state of uranium stems, in part, from the anticipated increase in the covalency of its metal–ligand interactions, relative to lower valent derivatives.<sup>28,29</sup> The presence of covalency in actinide bonding has previously been the subject of debate,<sup>30</sup> but the study of  $UO_2^{2+}$  over the past decade has convincingly demonstrated that the actinides can form covalent interactions.<sup>1,31</sup> However, the extent of covalency in the actinides is still not well understood, and studying the bonding in the f elements continues to be an active area of research.<sup>32–35</sup>

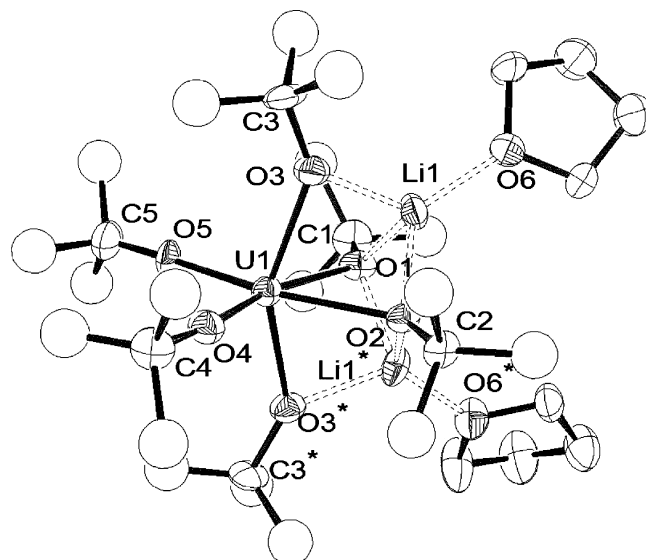


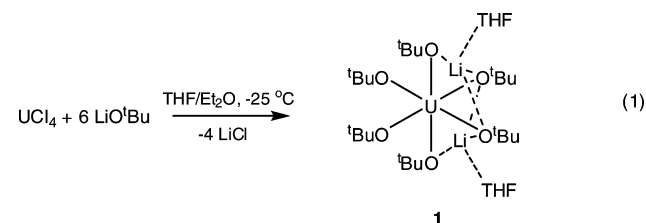
**Figure 1.** ORTEP diagram of  $[Li(THF)_2][U(O^tBu)_6]$  (**1**) with 30% probability ellipsoids. Asterisks indicate symmetry-related atoms. Selected bond lengths (Å) and angles (deg): U1–O1 = 2.384(9), U1–O2 = 2.412(8), U1–O3 = 2.252(6), U1–O4 = 2.137(9), U1–O5 = 2.140(8), Li1–O1 = 1.97(2), Li1–O2 = 2.02(2), Li1–O3 = 2.05(2), Li1–O6 = 1.96(2), U1–O1–C1 = 135.0(9), U1–O2–C2 = 131.3(8), U1–O3–C3 = 139.9(6), U1–O4–C4 = 171.3(9), U1–O5–C5 = 176(1), O3–U1–O3\* = 150.1(3), O1–U1–O5 = 97.3(3), O2–U1–O5 = 162.2(3).

In this contribution, we describe the synthesis, and characterization of three homoleptic alkoxides of uranium, namely  $[Li(THF)_2][U(O^tBu)_6]$ ,  $[Li(Et_2O)][U(O^tBu)_6]$ , and  $U(O^tBu)_6$ , which differ only in the oxidation state of the uranium center. In addition, we have studied the solution-phase behavior of  $[Li(THF)_2][U(O^tBu)_6]$ , and have observed its decomposition to the dinuclear uranium(IV) complex,  $[Li(THF)][U_2(O^tBu)_9]$ . This species is isostructural to the potassium analogue yet is thermally stable at room temperature. All compounds have been fully characterized by X-ray crystallography and  $^1H$  and  $^7Li\{^1H\}$  NMR spectroscopies, while  $U(O^tBu)_6$  has also been studied by cyclic voltammetry.

## Results and Discussion

### Synthesis and Characterization of $[Li(THF)_2][U(O^tBu)_6]$ .

The reaction of  $UCl_4$  with 6 equiv of  $LiO^tBu$  in THF/ $Et_2O$  at  $-25$  °C produces a blue solution containing  $[Li(THF)_2][U(O^tBu)_6]$  (**1**), which can be isolated in 61% yield as blue hexagonal plates (eq 1).



Single crystals of **1** suitable for X-ray crystallography were grown by evaporation of a dilute  $Et_2O$  solution over the course of several days. **1** crystallizes in the orthorhombic space group  $Pnma$ , and its solid-state molecular structure is shown in Figure 1. The solid-state molecular structure of **1** reveals a distorted octahedral geometry around uranium (e.g.,

- (19) Jacob, E. *Angew. Chem., Int. Ed. Engl.* **1982**, *21*, 142–143.  
 (20) Marks, T. J.; Cuellar, E. A. *Inorg. Chem.* **1981**, *20*, 2129–2137.  
 (21) Marks, T. J.; Cuellar, E. A. *J. Am. Chem. Soc.* **1983**, *105*, 4580–4589.  
 (22) Marks, T. J.; Bursten, B. E.; Casarin, M.; Ellis, D. E.; Fragala, I. *Inorg. Chem.* **1986**, *25*, 1257–1261.  
 (23) Cotton, F. A.; Marler, D. O.; Schwotzer, W. *Inorg. Chim. Acta* **1984**, *85*, L31–L32.  
 (24) Cotton, F. A.; Marler, D. O.; Schwotzer, W. *Inorg. Chem.* **1984**, *23*, 4211–4215.  
 (25) Van Der Sluys, W. G.; Sattelberger, A. P.; McElfresh, M. W. *Polyhedron* **1990**, *9*, 1843–1848.  
 (26) Van Der Sluys, W. G.; Fleig, P. F.; Berg, J. M. *Inorg. Chim. Acta* **1993**, *211*, 243–246.  
 (27) Cotton, F. A.; Marler, D. O.; Schwotzer, W. *Inorg. Chim. Acta* **1984**, *95*, 207–209.  
 (28) Mingos, D. M. P. *Essential Trends in Inorganic Chemistry* Oxford University Press: New York, NY, 1998.  
 (29) Choppin, G. R. *J. Alloys Compd.* **2002**, *344*, 55–59.  
 (30) Raymond, K. N.; Eigenbrot, C. W. *Acc. Chem. Res.* **1980**, *13*, 276–283.  
 (31) Denning, R. G. *Struct. Bonding (Berlin)* **1992**, *79*, 215–276.  
 (32) Gaunt, A. J.; Reilly, S. D.; Enriquez, A. E.; Scott, B. L.; Ibers, J. A.; Sekar, P.; Ingram, K. I. M.; Kaltsoyannis, N.; Neu, M. P. *Inorg. Chem.* **2008**, *47*, 29–41.  
 (33) Miguiditchian, M.; Guillauneux, D.; Guillaumont, D.; Moisy, P.; Madic, C.; Jensen, M. P.; Nash, K. L. *Inorg. Chem.* **2005**, *44*, 1404–1412.  
 (34) Mazzanti, M.; Wietzke, R.; Pecaut, J.; Latour, J. M.; Maldivi, P.; Remy, M. *Inorg. Chem.* **2002**, *41*, 2389–2399.  
 (35) Jensen, M. P.; Bond, A. H. *J. Am. Chem. Soc.* **2002**, *124*, 9870–9877.

O3–U1–O3\* = 150.1(3)°. The two lithium cations are tightly packed within the secondary coordination sphere, and each is bound in a pocket formed by the oxygen atoms of three *tert*-butoxide ligands. The coordination sphere of each lithium also includes one THF molecule, resulting in an overall tetrahedral coordination environment for lithium. The U–O bond lengths range from U1–O4 = 2.137(9) Å to U1–O2 = 2.412(8) Å, whereas the U–O–C bond angles range from U1–O2–C2 = 131.3(8)° to U1–O5–C5 = 176(1)°. The *tert*-butoxide groups that are also coordinated to lithium exhibit longer U–O bond distances (e.g., U1–O2 = 2.412(8) Å) and smaller U–O–C bond angles (U1–O2–C2 = 131.3(8)°), when compared with the nonbridging alkoxides (U1–O4 = 2.137(9) Å, U1–O5 = 2.140(8) Å, U1–O4–C4 = 171.3(9)°, U1–O5–C5 = 176(1)°). These large U–O–C bond angles are suggestive of a U–O  $\pi$  interaction via donation of the oxygen lone pairs.<sup>36</sup> The U–O bond distances are comparable to other reported U(IV) alkoxide complexes,<sup>24,27,37–39</sup> whereas the Li–O(alkoxide) interactions (Li1–O1 = 1.97(2) Å, Li1–O2 = 2.02(2) Å, and Li1–O3 = 2.05(2) Å) are slightly longer than those in other lithium salts of uranium(IV) alkoxides, such as Li[MeU(OCH(*t*Bu)<sub>2</sub>)<sub>4</sub>] and [Li(THF)][UN(CH<sub>2</sub>CH<sub>2</sub>–NSiMe<sub>3</sub>)<sub>3</sub>(O*t*Bu)<sub>2</sub>],<sup>38,39</sup> but are typical of heterometallic alkoxides containing lithium.<sup>40</sup>

The structures of several homoleptic uranium(IV) aryloxide complexes have also been determined and they exhibit U–O bond lengths ranging from 2.132(8) Å to 2.19(2) Å, similar to the U–O bond lengths observed in **1**.<sup>41–44</sup> Several homoleptic amido and alkyl complexes of uranium(IV) have also been reported, specifically [Li(THF)]<sub>2</sub>[U(NMe<sub>2</sub>)<sub>6</sub>], and Li<sub>2</sub>[UR<sub>6</sub>] [R = Me, Ph, CH<sub>2</sub>SiMe<sub>3</sub>], but these complexes have not been structurally characterized.<sup>45,46</sup> Interestingly, the isostructural cerium(IV) analogue of **1** is also known, namely [Na(DME)]<sub>2</sub>[Ce(O*t*Bu)<sub>6</sub>].<sup>47</sup> This complex exhibits remarkably similar terminal alkoxide M–O–C bond angles (172.5(4)° and 172.8(4)°) and M–O bond lengths (2.136(4) Å and 2.146(4) Å) to **1**. This structural similarity may arise from the comparable ionic radii of uranium(IV) and cerium(IV) (0.89 Å and 0.87 Å, respectively).<sup>48</sup>

The <sup>1</sup>H NMR spectrum of **1** in THF-*d*<sub>8</sub> at room temperature displays a broad resonance at 1.51 ppm, which we have assigned to the *tert*-butyl groups, whereas a single peak is observed in its <sup>7</sup>Li{<sup>1</sup>H} NMR spectrum at 2.72 ppm. These spectra suggest that the two lithium cations are either completely solvated under these conditions, or are contained within the secondary coordination sphere, but are exchanging rapidly between the binding sites formed by the alkoxide oxygens. Solutions of **1** are stable in THF-*d*<sub>8</sub> with no appreciable decomposition observed after 1 week at room temperature.

In contrast, the NMR spectra of **1** in C<sub>6</sub>D<sub>6</sub> are much more complicated. For instance, its <sup>1</sup>H NMR spectrum contains three broad singlets at 1.31, 1.90, and 2.40 ppm, which we have assigned to the *tert*-butyl substituents, while the signals for the coordinated THF ligands are observed at 1.25 and 3.16 ppm. The <sup>7</sup>Li{<sup>1</sup>H} NMR spectrum of **1** in C<sub>6</sub>D<sub>6</sub> consists of two broad resonances at –0.91 ppm and –1.66 ppm, neither of which are assignable to free LiO*t*Bu.<sup>49</sup> Interestingly, upon the addition of 20 equiv of THF to these samples the three *tert*-butyl resonances in the <sup>1</sup>H NMR spectrum coalesce into one peak, replicating the spectrum observed in THF-*d*<sub>8</sub>. A similar change is also observed in the <sup>7</sup>Li{<sup>1</sup>H} NMR spectrum. Solutions of **1** in toluene-*d*<sub>8</sub> are qualitatively similar to those observed in C<sub>6</sub>D<sub>6</sub>. Upon warming these solutions, the three *tert*-butyl resonances gradually coalesce, and at 60 °C only a single peak at 1.64 ppm is observed for the *tert*-butoxide ligands in the <sup>1</sup>H NMR spectrum. Similarly, upon warming to 60 °C an upfield shift of the resonances is observed in the <sup>7</sup>Li{<sup>1</sup>H} NMR spectra, from –0.91 ppm and –1.66 ppm, to –2.06 ppm and –3.74 ppm, respectively, while the relative intensities of these resonances also change as the signal at –2.06 ppm nearly disappears. Data at higher temperatures could not be collected because of the decomposition of **1**.

The complexity of the <sup>1</sup>H and <sup>7</sup>Li{<sup>1</sup>H} NMR spectra in C<sub>6</sub>D<sub>6</sub> may reflect the presence of multiple isomers in solution that interchange slowly under ambient conditions. For example, the broad resonance at 1.90 ppm in the <sup>1</sup>H NMR spectrum could be attributed to the structure observed in the solid state, but where rotation of the two lithium cations about the *tert*-butoxide pockets is occurring. This would make all six *tert*-butoxide ligands magnetically equivalent. The other two resonances in the <sup>1</sup>H NMR spectrum could be attributed to an isomer in which one lithium cation is solvated by four THF ligands and is no longer coordinated by a *tert*-butoxide binding pocket, which could occur if a small amount of residual THF was present in the sample. Such a structure, if static, should exhibit two peaks in its <sup>1</sup>H NMR spectrum in a 1:1 ratio, which fits with the observed spectrum. Interestingly, [Li(THF)<sub>4</sub>]<sup>+</sup> is reported to exhibit a <sup>7</sup>Li chemical shift of –1.05 ppm,<sup>50</sup> close to the chemical shift observed for one of the peaks in the <sup>7</sup>Li NMR spectrum of **1**. In addition,

(36) Crabtree, R. H. *The Organometallic Chemistry of the Transition Metals*, 3rd ed.; John Wiley & Sons, Inc.: New York, NY, 2001.

(37) Ephritikhine, M.; Baudin, C.; Baudry, D.; Lance, M.; Navaza, A.; Nierlich, M.; Vigner, J. *J. Organomet. Chem.* **1991**, *415*, 59–63.

(38) Andersen, R. A.; Stewart, J. L. *J. Chem. Soc., Chem. Commun.* **1987**, 1846–1847.

(39) Scott, P.; Roussel, P.; Hitchcock, P. B.; Tinker, N. D. *Inorg. Chem.* **1997**, *36*, 5716–5721.

(40) Snaith, R.; Wright, D. S., *Complexes of Inorganic Lithium Salts. In Lithium Chemistry: A Theoretical and Experimental Overview*, Sapsee, A.-M.; von Rague Schleyer, P., Eds. John Wiley & Sons, Inc: New York, 1995; pp 227–293.

(41) Van Der Sluys, W. G.; Sattelberger, A. P. *Polyhedron* **1989**, *8*, 1247–1249.

(42) Lappert, M. F.; Blake, P. C.; Taylor, R. G. *Inorg. Chim. Acta* **1987**, *139*, 303–315.

(43) Clark, D. L.; Berg, J. M.; Huffman, J. C.; Morris, D. E.; Sattelberger, A. P.; Streib, W. E.; Van Der Sluys, W. G.; Watkin, J. G. *J. Am. Chem. Soc.* **1992**, *114*, 10811–10821.

(44) Clark, D. L.; Sattelberger, A. P.; Van Der Sluys, W. G. *J. Alloys Compd.* **1992**, *180*, 303–315.

(45) Ephritikhine, M.; Berthet, J. C. *Coord. Chem. Rev.* **1998**, *178–180*, 83–116.

(46) Wilkinson, G.; Sigurdson, E. R. *J. Chem. Soc., Dalton Trans.* **1977**, 812–818.

(47) Evans, W. J.; Deming, T. J.; Olofson, J. M.; Ziller, J. W. *Inorg. Chem.* **1989**, *28*, 4027–4034.

(48) Shannon, R. D. *Acta Crystallogr., Sect. A* **1976**, *A32*, 751–767.

(49) The <sup>7</sup>Li resonance for free LiO*t*Bu in C<sub>6</sub>D<sub>6</sub> is observed at 0.86 ppm.

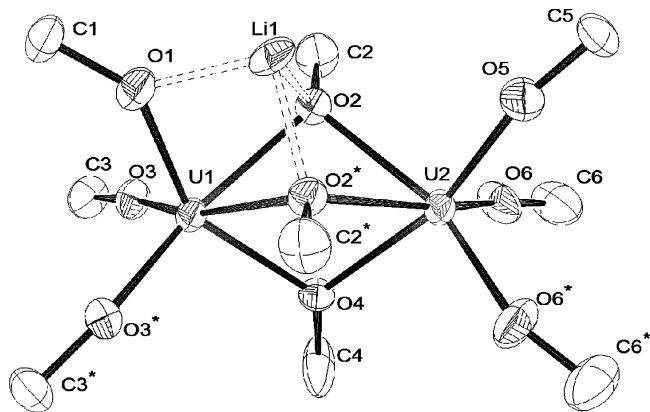


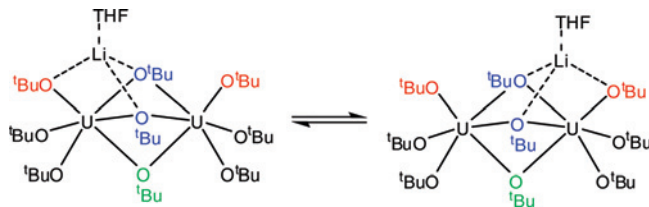
**Figure 2.** ORTEP diagram of  $[\text{Li}(\text{THF})][\text{U}(\text{O}^t\text{Bu})_9] \cdot \text{C}_5\text{H}_{12}$  ( $2 \cdot \text{C}_5\text{H}_{12}$ ) with 50% probability ellipsoids. The methyl groups and the THF coordinated to the lithium cation have been excluded for clarity. Asterisks indicate symmetry-related atoms. Selected bond lengths (Å) and angles (deg): U1–O1 = 2.221(9), U1–O2 = 2.494(6), U1–O3 = 2.108(6), U1–O4 = 2.346(9), U2–O2 = 2.498(6), U2–O4 = 2.431(8), U2–O5 = 2.12(1), U2–O6 = 2.128(7), Li1–O1 = 2.00(3), Li1–O2 = 2.06(2), Li1–O7 = 1.95(3), U1–U2 = 3.6845(7), U1–O1–C1 = 140.0(8), U1–O2–C2 = 125.2(6), U1–O3–C3 = 171.1(7), U1–O4–C4 = 128.6(7), U2–O5–C5 = 167(1), U2–O6–C6 = 159.7(8), U1–O2–U2 = 95.1(2), U1–O4–U2 = 100.9(3).

rapid exchange of the THF ligands coordinated to lithium could account for the observation of only one set of THF resonances in the  $^1\text{H}$  NMR spectrum. Subsequent addition of THF or heat could allow these isomers to exchange rapidly or alternatively stabilizes one structure over the other.

When solutions of **1** in  $\text{C}_6\text{D}_6$  are allowed to stand over the course of several hours, new signals begin to appear in the  $^1\text{H}$  and  $^7\text{Li}\{^1\text{H}\}$  NMR spectra. In particular, two new peaks appear in the  $^7\text{Li}\{^1\text{H}\}$  NMR spectrum at  $-7.19$  and  $-28.80$  ppm. On a preparative scale, when a suspension of **1** is stirred in hexanes, the solid slowly dissolves and the color changes from light-blue to green. The rate at which the change occurs is dependent on starting concentration and temperature, but conversion is typically complete after 6 h. Single crystals isolated from the slow evaporation of these solutions at  $-25$  °C result in the isolation of a dinuclear uranium(IV) complex,  $[\text{Li}(\text{THF})][\text{U}_2(\text{O}^t\text{Bu})_9]$  (**2**).

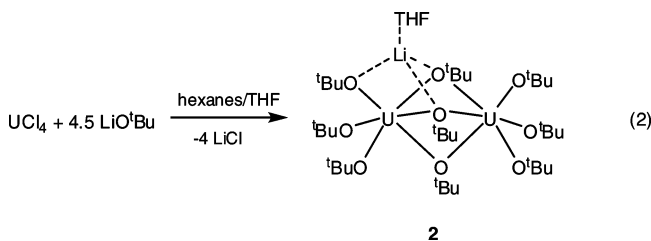
**2** crystallizes in the monoclinic space group  $C2/m$  as a pentane solvate,  $2 \cdot \text{C}_5\text{H}_{12}$  (Figure 2). **2** consists of two uranium centers in a face-sharing octahedral coordination environment, which results in six terminal alkoxide ligands and three bridging alkoxide ligands. In addition, a lithium cation occupies a pocket formed by one terminal alkoxide and two bridging alkoxides. The coordination sphere of lithium also includes one molecule of THF, giving the lithium ion a tetrahedral geometry. The U–O bond distances in  $2 \cdot \text{C}_5\text{H}_{12}$  is similar to those observed in **1** and similar to those observed for the nearly isostructural molecule,  $\text{K}[\text{U}_2(\text{O}^t\text{Bu})_9]$ .<sup>24</sup> For instance, the terminal alkoxide U–O bond lengths in  $2 \cdot \text{C}_5\text{H}_{12}$  are U1–O3 = 2.108(6) Å, U2–O5 = 2.12(1) Å, and U2–O6 = 2.128(7) Å, whereas those in  $\text{K}[\text{U}_2(\text{O}^t\text{Bu})_9]$  range from 2.10(2) to 2.14(2) Å. As anticipated, the U–O bond lengths of the bridging alkoxide ligands (U1–O2 = 2.494(6) Å, U1–O4 = 2.346(9) Å, U2–O2 = 2.498(6) Å, U2–O4 = 2.431(8) Å) are longer than those of the terminal alkoxides, while the Li–O(alkoxide) bond

Scheme 1



lengths (Li1–O1 = 2.00(3) Å, Li1–O2 = 2.06(2) Å) are similar to those observed in **1**. In addition, **2** exhibits large U–O–C bond angles (U1–O3–C3 = 171.1(7)°, U2–O5–C5 = 167(1)°, U2–O6–C6 = 159.7(8)°) for the terminal alkoxide ligands. A cerium(IV) analogue to complex **2**,  $\text{Na}[\text{Ce}_2(\text{O}^t\text{Bu})_9]$ , has also been reported, which further illustrates the similarities between uranium(IV) and cerium(IV) alkoxide chemistry.<sup>47</sup>

A rational synthesis of **2** can be achieved by addition of 4.5 equiv of  $\text{LiO}^t\text{Bu}$  to  $\text{UCl}_4$  in a hexanes/THF solution (5:1 ratio) at room temperature (eq 2). By this route **2** can be isolated in 54% yield.



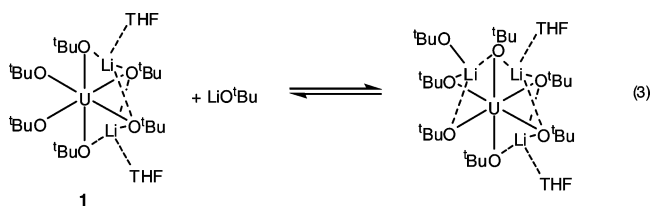
The  $^7\text{Li}\{^1\text{H}\}$  NMR spectrum of **2** in  $\text{C}_6\text{D}_6$ , containing trace amounts of THF, consists of a singlet at  $-28.80$  ppm, which matches one of the two extraneous signals observed upon decomposition of **1**. The  $^1\text{H}$  NMR spectrum of **2** is both highly solvent and temperature dependent. In  $\text{C}_6\text{D}_6$  or toluene- $d_8$  at room temperature, its spectrum appears as three broad, featureless peaks. However, cooling a toluene- $d_8$  solution of **2** to  $-15$  °C generates a  $^1\text{H}$  NMR spectrum consisting of four sharp singlets in a 4:2:2:1 ratio, while an upfield shift is observed for the resonance in the  $^7\text{Li}\{^1\text{H}\}$  NMR spectrum, from  $-17.87$  to  $-33.48$  ppm. In addition, warming a toluene- $d_8$  solution of **2** to 70 °C causes the three broad peaks in the  $^1\text{H}$  NMR spectrum to coalesce into one broad resonance observed at 1.52 ppm. Finally, the room temperature  $^1\text{H}$  NMR spectrum of **2** in THF- $d_8$  mirrors the spectrum observed in toluene- $d_8$  at  $-15$  °C. The 4:2:2:1 pattern observed in the THF and toluene- $d_8$  NMR spectra can be easily explained by assuming facile exchange of the lithium cation between the two available binding pockets, formed by two bridging and one terminal alkoxide ligand, which are found on one face of the complex (Scheme 1). Upon warming these solutions, it could be imagined that exchange of bridging and terminal alkoxides could then occur, which would make all nine alkoxide ligands magnetically equivalent.

Interestingly, the potassium analogue,  $\text{K}[\text{U}_2(\text{O}^t\text{Bu})_9]$ , is unstable above 5 °C and spontaneously converts to the mixed-valent uranium complex,  $\text{U}_2(\text{O}^t\text{Bu})_9$ , upon standing.<sup>24</sup> In contrast, **2** appears to be stable in THF at room tem-

perature and does not appear to convert to  $U_2(O^tBu)_9$ . We have also observed the presence of  $U_3(O)(O^tBu)_{10}$  in solutions of **2**. This complex has been observed by Cotton and others<sup>23–25,27</sup> and is likely formed by the reaction of **2** with trace amounts of water.<sup>25,51</sup>

We have performed several experiments to elucidate the nature of the other species formed upon decomposition of **1**, which is responsible for the singlet observed at  $-7.19$  ppm in the  $^7Li\{^1H\}$  NMR spectrum. Addition of excess  $LiO^tBu$  to a  $C_6D_6$  solution of **1** gives rise to a new signal at  $-7.19$  ppm in the  $^7Li\{^1H\}$  NMR spectrum. The signals at  $-0.91$  and  $-1.66$  ppm are still observable, however the intensity of the peak at  $-0.91$  ppm decreases relative to the peak at  $-1.66$  ppm. Notable changes also occur in the  $^1H$  NMR spectra of these samples. Of the three *tert*-butoxide signals attributed to **1** in  $C_6D_6$ , addition of  $LiO^tBu$  causes two resonances ( $1.31$  ppm and  $2.40$  ppm) to sharpen in intensity whereas the third ( $1.90$  ppm) broadens significantly.

Given these results, we propose that **1** forms an adduct with  $LiO^tBu$ , namely  $1 \cdot LiO^tBu$ , in which the lithium cation of the incoming  $LiO^tBu$  can bind to an unoccupied pocket formed by three alkoxide ligands (eq 3). As there is only one signal observed in the  $^7Li\{^1H\}$  NMR spectrum for the adduct, rapid exchange between the alkoxide pockets may be occurring. In contrast, similar titration experiments in THF- $d_8$  do not result in the formation of any new species as determined by  $^1H$  and  $^7Li\{^1H\}$  NMR spectroscopy. In this case, coordination of THF to the lithium cation of  $LiO^tBu$  probably prevents capture by **1**. Thus far, all attempts at isolating the  $LiO^tBu$  adduct of **1** have proven unsuccessful and result in the isolation of mixtures of **1** and  $LiO^tBu$ .



Interestingly, addition of  $LiCl$  to a solution of **1** in  $C_6D_6$  also results in the formation of a new peak in the  $^7Li\{^1H\}$  NMR spectrum, at  $-7.23$  ppm. Given that  $LiCl$  is not appreciably soluble in benzene, the presence of this new peak is most likely the result of  $LiCl$  capture by **1**, and provides further support for the formation of  $1 \cdot LiO^tBu$ . The ability of lithium “ate” complexes to incorporate lithium halides into their structures is well established.<sup>40</sup>

The formation of **2** from **1** in  $C_6D_6$  requires the production of uncomplexed  $LiO^tBu$ . Yet, the presence of free  $LiO^tBu$  is not observed in either the  $^1H$  or  $^7Li\{^1H\}$  NMR spectra. Furthermore, in the presence of excess  $LiO^tBu$ , samples of **2** (independently prepared from  $UCl_4$ ) in  $C_6D_6$  slowly convert back to **1** over the course of 12 h at room temperature. To account for these observations and the

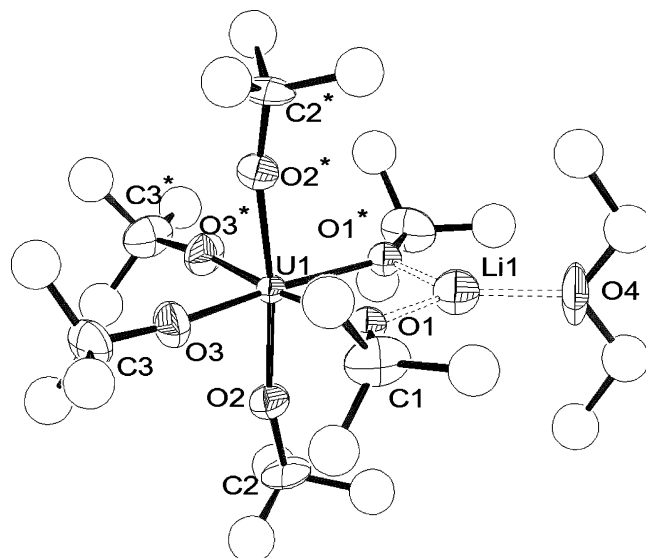
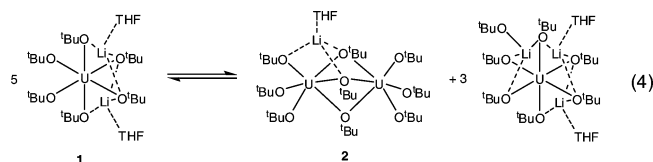


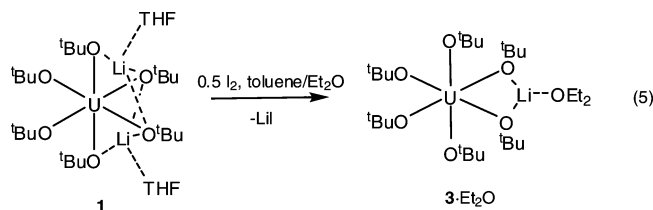
**Figure 3.** ORTEP diagram of  $[Li(Et_2O)][U(O^tBu)_6]$  (**3**· $Et_2O$ ) with 30% probability ellipsoids. Asterisks indicate symmetry-related atoms. Selected bond lengths (Å) and angles (deg): U1–O1 = 2.24(1), U1–O2 = 2.059(9), U1–O3 = 2.05(1), Li1–O1 = 1.91(3), Li1–O4 = 1.93(4), U1–O1–C1 = 140(1), U1–O2–C2 = 167(3), U1–O3–C3 = 167(1), O1–U1–O2 = 92.8(7), O1–U1–O3 = 94.2(5), O1–U1–O3\* = 171.0(6), O2–U1–O2\* = 173(2), O2–U1–O3 = 87.6(6).

results summarized in eq 3, we propose that **1**, **2**, and  $1 \cdot LiO^tBu$  are in equilibrium and that the  $LiO^tBu$  generated upon formation of **2** can react with **1** to form the adduct  $1 \cdot LiO^tBu$  (eq 4).



### Synthesis and Characterization of $[Li(Et_2O)][U(O^tBu)_6]$ .

We have also explored the redox chemistry of **1**. Addition of 0.5 equiv of  $I_2$  to **1** in toluene at room temperature generates a pale-yellow solution, which affords a white powder upon solvent removal. Recrystallization of this material from diethyl ether affords  $[Li(Et_2O)][U(O^tBu)_6]$  (**3**· $Et_2O$ ) as pale-yellow hexagonal plates in 25% yield (eq 5).



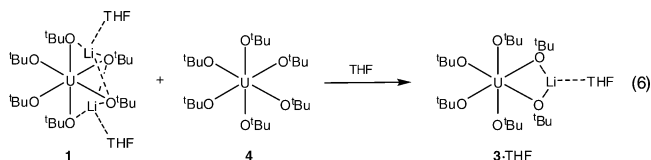
**3**· $Et_2O$  crystallizes in the orthorhombic space group *Imm*2, and its solid-state molecular structure is presented in Figure 3. This molecule possesses a nearly octahedral geometry (O1–U1–O2 = 92.8(7)°, O2–U1–O3 = 87.6(6)°, O2–U1–O2\* = 173(2)°, O1–U1–O3\* = 171.0(6)°). The lithium cation is contained within the secondary coordination sphere and is ligated by two *tert*-butoxide ligands and one diethyl ether molecule affording it a trigonal planar geometry.

(50) Barley, H. R. L.; Clegg, W.; Dale, S. H.; Hevia, E.; Honeyman, G. W.; Kennedy, A. R.; Mulvey, R. E. *Angew. Chem., Int. Ed.* **2005**, *44*, 6018–6021.

(51) Leverd, P.; Nierlich, M. *Eur. J. Inorg. Chem.* **2000**, 1733–1738.

As anticipated, the U–O bonds in  $3 \cdot \text{Et}_2\text{O}$  (U1–O1 = 2.24(1) Å, U1–O2 = 2.059(9) Å, U1–O3 = 2.05(1) Å) are generally shorter than those observed in **1** and **2**, consistent with the smaller  $\text{U}^{5+}$  ionic radius. In addition, the nonbridging alkoxides exhibit shorter U–O bonds than the bridging alkoxides, identical to the trend seen in **1** and **2**. The nonbridging alkoxide ligands exhibit nearly linear U–O–C bond angles (U1–O2–C2 = 167(3)°, U1–O3–C3 = 167(1)°), whereas the bridging alkoxides possess the smallest U–O–C bond angle (U1–O1–C1 = 140(1)°). The observed bond length between lithium and the oxygen of the bridging alkoxide in  $3 \cdot \text{Et}_2\text{O}$  is 1.91(3) Å, while the Li–O( $\text{Et}_2\text{O}$ ) bond length is unremarkable (Li1–O4 = 1.93(4) Å) and is comparable to the Li–O(THF) bond distances observed in **1** and **2**. The only other structurally characterized U(V) alkoxide,  $[\text{U}(\text{O}^i\text{Pr})_5]_2$ , exhibits U–O bond lengths of 2.03(1) Å and 2.29(1) Å for the terminal and bridging alkoxides, respectively,<sup>24</sup> which are comparable to those observed in  $3 \cdot \text{Et}_2\text{O}$ .

The  $^1\text{H}$  NMR spectrum of  $3 \cdot \text{Et}_2\text{O}$  shows one large singlet for the *tert*-butoxide groups at 2.00 ppm in  $\text{C}_6\text{D}_6$ , suggesting rapid exchange of the lithium cation about all of the possible binding pockets. Its  $^7\text{Li}\{^1\text{H}\}$  NMR spectrum consists of one peak at 6.75 ppm. Furthermore, addition of THF to  $3 \cdot \text{Et}_2\text{O}$  displaces the coordinating diethyl ether to give  $[\text{Li}(\text{THF})][\text{U}(\text{O}^i\text{Bu})_6]$  ( $3 \cdot \text{THF}$ ). **3** is soluble in polar organic solvents such as THF and diethyl ether, sparingly soluble in toluene or  $\text{C}_6\text{D}_6$ , and is stable in these solvents at room temperature. Unfortunately, both **3** and the LiI generated upon oxidation have similar solubility properties, and the separation of the two becomes problematic in larger scale reactions. This problem can be avoided through the comproportionation of **1** and the uranium(VI) complex  $\text{U}(\text{O}^i\text{Bu})_6$  (vide infra) in THF, which provides a lithium iodide-free method for the generation of  $3 \cdot \text{THF}$  (eq 6). Interestingly,  $\text{U}(\text{OEt})_5$  has been similarly generated by comproportionation of  $\text{U}(\text{OEt})_6$  and  $\text{U}(\text{OEt})_4$ .<sup>11</sup>



The interaction of the lithium ion with the *tert*-butoxide ligands appears critical to the stability of both **1** and **3**, and attempts to exchange the lithium cation for the noncoordinating tetraethylammonium ion have proven unsuccessful. Addition of  $[\text{NEt}_4]\text{Cl}$  to solutions of **1** or **3** results in a rapid color change to yellow, but these mixtures have proven intractable. It is possible that tight coordination of  $\text{Li}^+$  is required to offset the negative charge of the complex. Interestingly, many of the uranium(V) alkoxide complexes that have already been isolated also contain a highly electropositive cation. For instance, Gilman has reported the synthesis and isolation of  $\text{Na}[\text{U}(\text{OC}_2\text{H}_5)_6]$ ,  $\text{Ca}[\text{U}(\text{OC}_2\text{H}_5)_6]_2$ , and  $\text{Al}[\text{U}(\text{OC}_2\text{H}_5)_6]_3$ .<sup>10</sup>

**Synthesis and Characterization of  $\text{U}(\text{O}^i\text{Bu})_6$ .** Pentane solutions of **1** are readily oxidized to uranium(VI) by the

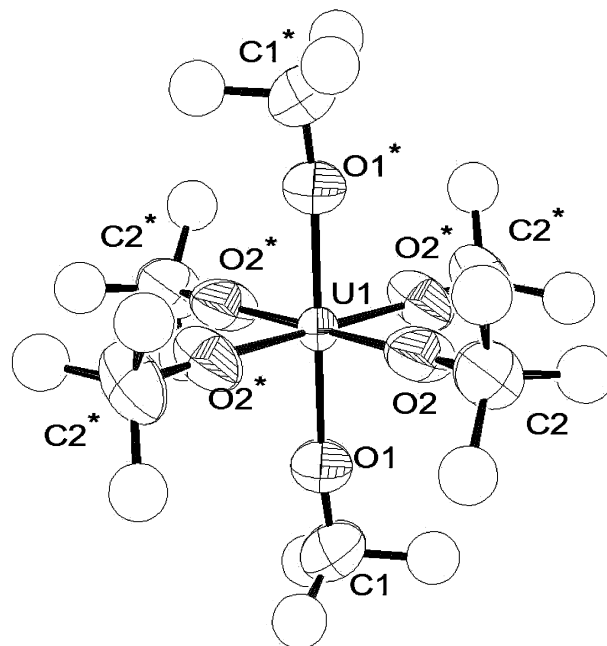
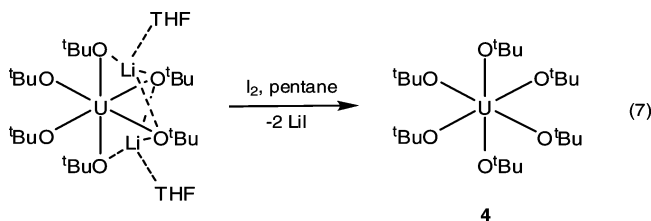


**Figure 4.** ORTEP diagram of one of two molecules present in the asymmetric unit of  $\text{U}(\text{O}^i\text{Bu})_6$  (**4**) with 30% probability. Asterisks indicate symmetry-related atoms. Selected bond lengths (Å) and angles (deg): U1–O1 = 2.05(1), U1–O2 = 2.027(8), U1–O1–C1 = 174(2), U1–O2–C2 = 175(1), O1–U1–O2 = 90.3(4).

addition of 1 equiv of  $\text{I}_2$  at room temperature. Subsequent filtration of the solution and removal of the solvent yields a dark-red solid. Recrystallization of this material from pentane yields dark-red plates of  $\text{U}(\text{O}^i\text{Bu})_6$  (**4**) in 61% yield (eq 7). Interestingly, this complex was first prepared by Bradley and co-workers via disproportionation of uranyl *tert*-butoxide, and as a side product in the attempted synthesis of  $\text{U}(\text{O}^i\text{Bu})_4$ .<sup>15,16</sup>



**4** crystallizes in the monoclinic space group  $C2/m$ . An X-ray diffraction analysis reveals two independent half-molecules contained within the asymmetric unit, and one full molecule, generated by symmetry is shown in Figure 4. **4** adopts an octahedral geometry in the solid-state (O1–U1–O2 = 90.3(4)°, O1–U1–O1\* = 180°, O2–U1–O2\* = 180°). The U–O bond lengths (U1–O1 = 2.05(1) Å, U1–O2 = 2.027(8) Å) are shorter than those observed in **1** but comparable to those observed in  $3 \cdot \text{Et}_2\text{O}$ . They are also comparable to those reported for  $\text{U}(\text{OCH}_3)_6$  (U–O = 2.10 Å) and  $\text{U}[\text{OCH}_2\text{C}(\text{CH}_3)_3]_6$  (U–O = 2.001(8) and 2.00(1) Å),<sup>22,52</sup> while the near-linear U–O–C bond angles (U1–O1–C1 = 174(2)°, U1–O2–C2 = 175(1)°) are larger than those of either  $\text{U}(\text{OCH}_3)_6$  (av, U–O–C = 154°)

(52) Wilkerson, M. P.; Burns, C. J.; Dewey, H. J.; Martin, J. M.; Morris, D. E.; Paine, R. T.; Scott, B. L. *Inorg. Chem.* **2000**, *39*, 5277–5285.

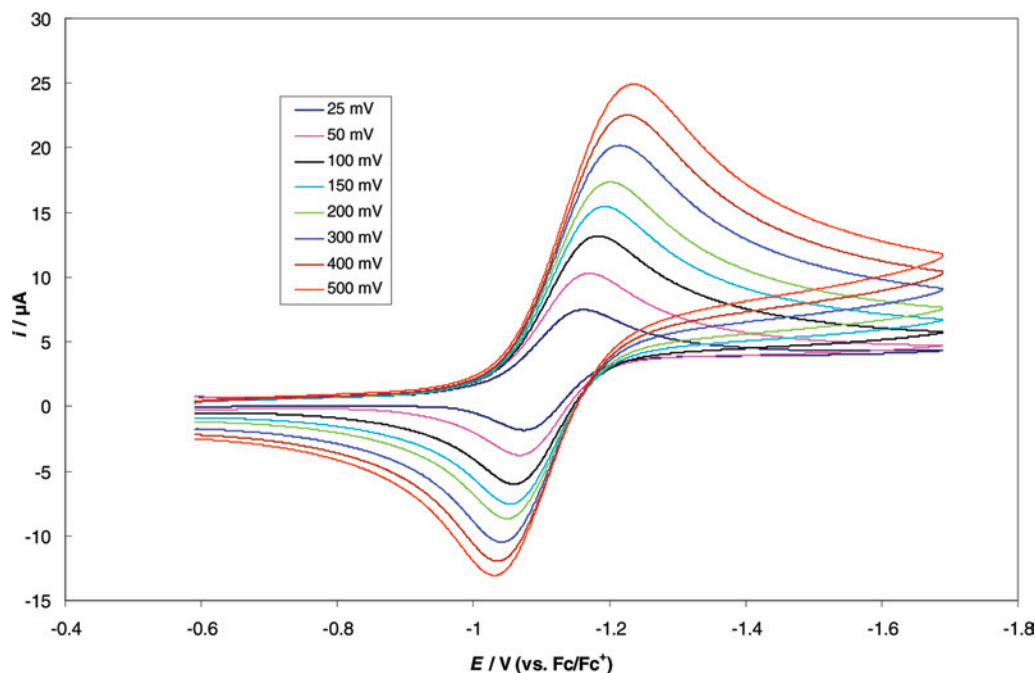


**Figure 5.** Room temperature cyclic voltammogram for **4** in  $\text{CH}_2\text{Cl}_2$  vs  $[\text{Cp}_2\text{Fe}]^{0/+}$  (0.1 M  $[\text{NBu}_4][\text{PF}_6]$  as supporting electrolyte).

or  $\text{U}[\text{OCH}_2\text{C}(\text{CH}_3)_3]_6$  (av,  $\text{U}-\text{O}-\text{C} = 146^\circ$ ), possibly because of the larger bulk of the *tert*-butyl group. Interestingly, the solid-state molecular structure of  $\text{W}(\text{OMe})_6$  has also been determined.<sup>53</sup> This complex exhibits an average  $\text{W}-\text{O}$  distance of 1.87 Å, roughly 0.18 Å shorter than the average  $\text{U}-\text{O}$  bond length observed for **4**. However, the  $\text{W}^{6+}$  ionic radius is 0.74 Å for C.N. = 6, which is 0.13 Å smaller than the value reported for  $\text{U}^{6+}$ .<sup>48</sup> This difference nearly accounts for the discrepancy in bond length between the two alkoxide complexes. Furthermore, the methoxide ligands in  $\text{W}(\text{OMe})_6$  are decidedly nonlinear, as the average  $\text{W}-\text{O}-\text{C}$  bond angle is  $121^\circ$ . The bent methoxide ligands are most likely an electronic manifestation because a similar structure is also observed in the gas phase.<sup>54</sup> The increased linearity of the alkoxide ligands of the homoleptic uranium complexes may be due to the availability of the 5f orbitals to accept electron density from the oxygen lone pairs, an orbital combination not possible in tungsten. Indeed, a theoretical study of  $\text{U}(\text{OMe})_6$  has demonstrated a significant 5f orbital contribution to the  $\pi$  framework of that molecule.<sup>22</sup>

The  $^1\text{H}$  NMR spectrum of **4** in  $\text{C}_6\text{D}_6$  exhibits a singlet for the *tert*-butyl substituents at 1.67 ppm, while recrystallized samples of **4** exhibit no signals in the  $^7\text{Li}\{^1\text{H}\}$  NMR spectrum. In contrast, the crude product displays a single peak in its  $^7\text{Li}\{^1\text{H}\}$  NMR spectrum at  $-2.25$  ppm, and this resonance is attributed to residual  $\text{LiI}$ , formed during the reaction of **1** with  $\text{I}_2$ . In support of this hypothesis, addition of  $\text{LiI}$  to a sample of pure  $\text{U}(\text{O}^t\text{Bu})_6$  results in the formation of a new signal at  $-2.25$  ppm in the  $^7\text{Li}\{^1\text{H}\}$  NMR spectrum over the course of several hours. Thus, it is likely that the alkoxy groups of **4** are able to chelate  $\text{LiI}$  as is observed in the interaction of  $\text{LiCl}$  and  $\text{Li}^t\text{OBu}$

with **1**. However, attempts to isolate the  $\text{LiI}$  adduct of **4** simply results in the recovery of  $\text{LiI}$  and  $\text{U}(\text{O}^t\text{Bu})_6$ .

**Electrochemical Studies.** We have attempted to determine the solution redox properties of **1**, **3**, and **4** by cyclic voltammetry. Unfortunately, the attempted electrochemical studies of **1** and  $\mathbf{3}\cdot\text{Et}_2\text{O}$  in  $\text{CH}_2\text{Cl}_2$ , with  $[\text{NBu}_4][\text{PF}_6]$  as supporting electrolyte, results in the immediate decomposition of these complexes. However, we have measured the cyclic voltammogram of **4** at room temperature in  $\text{CH}_2\text{Cl}_2$ . The cyclic voltammogram of this complex exhibits a reversible reduction feature at  $-1.12$  V (vs  $[\text{Cp}_2\text{Fe}]^{0/+}$ ) (Figure 5). For this feature,  $i_p/c/i_{p,a} \approx 1.1$  over the range of scan rates, up to 0.5 V/s, suggesting that the formation of the uranium(V) complex is chemically reversible. Further reduction of **4** to uranium(IV) was not observed within the range of the solvent window, whereas scanning to positive potentials produces two complex, irreversible oxidation features that presumably involve the removal of electrons from the *tert*-butoxide ligands.

The  $\text{U}(\text{VI})/\text{U}(\text{V})$  redox potential of **4** occurs at a similar potential observed for the uranium(V) hexakisamido complex,  $[\text{U}(\text{dbabh})_6]^-$  ( $\text{Hdbabh} = 2,3:5,6$ -dibenzo-7-azabicyclo[2.2.1]hepta-2,5-diene), ( $E_{1/2} = -1.01$  V vs.  $[\text{Cp}_2\text{Fe}]^{0/+}$ ).<sup>55</sup> The relatively small reduction potential of **4** contrasts with the reduction potential reported for  $\text{UF}_6$  ( $E_{1/2} = 2.31$  V vs.  $\text{Ag}/\text{Ag}^+$ ), which is a powerful oxidizing agent.<sup>56</sup> Similarly,  $\text{UCl}_6$  is reported to be a potent oxidant.<sup>4</sup> The observed reduction potential of **4** probably reflects the strong  $\pi$ -donating ability of the *tert*-butoxide ligands, which stabilizes the high oxidation state. This effect has also been noted in group 6 chemistry. For instance, the reduction potential of  $\text{WCl}_6$  was found to be 1.59 V (vs.

(53) Seisenbaeva, G. A.; Kloof, L.; Werndrup, P.; Kessler, V. G. *Inorg. Chem.* **2001**, *40*, 3815–3818.

(54) Haaland, A.; Rypdal, K.; Volden, H. V.; Jacob, E.; Weidlein, J. *Acta Chem. Scand.* **1989**, *43*, 911–913.

(55) Cummins, C. C.; Meyer, K.; Mindiola, D. J.; Baker, T. A.; Davis, W. M. *Angew. Chem., Int. Ed.* **2000**, *39*, 3063–3066.

(56) Winfield, J. M.; Andersen, G. M.; Iqbal, J.; Sharp, D. W. A.; Cameron, J. H.; McLeod, A. G. *J. Fluor. Chem.* **1984**, *24*, 303–317.

**Table 1.** X-ray Crystallographic Data for Complexes **1**, **2**·C<sub>5</sub>H<sub>12</sub>, **3**·Et<sub>2</sub>O, **4**

	<b>1</b>	<b>2</b> ·C <sub>5</sub> H <sub>12</sub>	<b>3</b> ·Et <sub>2</sub> O	<b>4</b>
empirical formula	C <sub>32</sub> H <sub>70</sub> Li <sub>2</sub> O <sub>8</sub> U	C <sub>40</sub> H <sub>89</sub> LiO <sub>10</sub> U <sub>2</sub> ·C <sub>5</sub> H <sub>12</sub>	C <sub>28</sub> H <sub>62</sub> LiO <sub>7</sub> U	C <sub>24</sub> H <sub>54</sub> O <sub>6</sub> U
crystal Habit, color	needle, blue	plate, green	hexagonal plate, pale yellow	needle, red
cryst size (mm)	0.2 × 0.08 × 0.05	0.25 × 0.2 × 0.02	0.4 × 0.4 × 0.1	0.07 × 0.07 × 0.03
cryst syst	orthorhombic	monoclinic	orthorhombic	monoclinic
space group	<i>Pnma</i>	<i>C2/m</i>	<i>Imm2</i>	<i>C2/m</i>
volume (Å <sup>3</sup> )	3964.8(9)	5662.6(9)	1829(7)	4649(2)
<i>a</i> (Å)	22.170(3)	41.314(4)	11.18(2)	28.536(6)
<i>b</i> (Å)	16.430(2)	11.064(1)	12.41(3)	16.791(3)
<i>c</i> (Å)	10.885(2)	12.646(1)	13.19(3)	9.725(2)
α (deg)	90	90	90	90
β (deg)	90	101.592(2)	90	93.80(3)
γ (deg)	90	90	90	90
<i>Z</i>	4	4	2	6
fw (g/mol)	834.79	1285.26	757.76	676.70
density <sub>calcd</sub> (Mg/m <sup>3</sup> )	1.399	1.508	1.376	1.450
absorption coefficient (mm <sup>-1</sup> )	4.134	5.758	4.471	5.266
<i>F</i> <sub>000</sub>	1696	2552	766	2028
total no. reflns	20 944	22 423	7142	19 563
unique reflns	4338	6041	2024	5097
final R indices ( <i>I</i> > 2σ( <i>I</i> ))	R1 = 0.0596, wR2 = 0.1326	R1 = 0.0565, wR2 = 0.1536	R1 = 0.0352 wR2 = 0.0873	R1 = 0.0537 wR2 = 0.1206
largest diff. peak and hole (e <sup>-</sup> Å <sup>-3</sup> )	3.380 and -2.731	2.850 and -1.091	1.319 and -2.075	1.602 and -1.311
GOF	0.874	1.046	1.083	0.911

SCE), whereas that of [W(N)Cl<sub>4</sub>]<sup>-</sup>, a complex containing the strongly π-donating nitride ligand, is much smaller (*E*<sub>1/2</sub> = -0.43 V vs. SCE).<sup>57</sup> Similarly, the limited oxidizing power of uranyl (UO<sub>2</sub><sup>2+</sup>) can be attributed to the strong π-donating ability of its oxo ligands.<sup>4</sup> The tempered oxidizing power of **4** is also evident in its method of synthesis, which only requires the mild oxidant I<sub>2</sub> to achieve the 6+ oxidation state.

## Summary

Isolation of the homoleptic, octahedral uranium(IV) alkoxide [Li(THF)<sub>2</sub>U(O'Bu)<sub>6</sub>] can be achieved by reaction of UCl<sub>4</sub> and 6 equiv of LiO'Bu. It is notable that previous synthetic efforts with the *tert*-butoxide ligand did not uncover the octahedral derivative.<sup>7,9,23–26</sup> Presumably, our use of the lithium salt of *tert*-butoxide makes this species stable, as the ability of lithium to tightly bind the secondary coordination sphere of the uranium probably overcomes the destabilization that arises from the dianionic charge that the uranium center formally possesses. The use of a “softer” cation would most likely preclude the coordination of the six *tert*-butoxides required to form the homoleptic octahedral species. However, [Li(THF)<sub>2</sub>U(O'Bu)<sub>6</sub>] is only kinetically stable, and it exhibits a complicated solution-phase behavior in C<sub>6</sub>D<sub>6</sub>, where it slowly decomposes, forming a dinuclear uranium(IV) species, [Li(THF)]<sub>2</sub>[U<sub>2</sub>(O'Bu)<sub>9</sub>]. The LiO'Bu generated during dimerization is likely captured by the remaining [Li(THF)<sub>2</sub>U(O'Bu)<sub>6</sub>] to form an LiO'Bu adduct, [Li(THF)<sub>2</sub>U(O'Bu)<sub>6</sub>]·LiO'Bu. Irrespective of its instability, [Li(THF)<sub>2</sub>U(O'Bu)<sub>6</sub>] has proven to be a useful starting material, and addition of 0.5 or 1 equiv of I<sub>2</sub> generates the uranium(V) and uranium(VI) complexes, [Li(Et<sub>2</sub>O)]<sub>2</sub>[U(O'Bu)<sub>6</sub>] and U(O'Bu)<sub>6</sub>, respectively, in good yields. Characterization of these two complexes by X-ray crystallography has shown that they possess large U–O–C bond angles, suggesting the presence of a π interaction between

the oxygen lone pairs and the uranium metal center. Finally, the isolation of **1**, **3**, and **4** provides us with the opportunity to systematically study the chemistry of three homoleptic uranium alkoxides, differing only in their oxidation state. We plan to further examine the bonding interactions in these compounds, particularly the interaction of the 5f orbitals and the oxygen-based lone-pairs. **1**, **3**, and **4** should also be versatile starting materials, and future work will focus on their elaboration via protonolysis.

## Experimental Section

**General.** All reactions and subsequent manipulations were performed under anaerobic and anhydrous conditions either under a high vacuum or an atmosphere of argon inside a Vacuum Atmospheres OMNI-LAB glovebox. Diethyl ether, toluene, hexanes, and tetrahydrofuran were purchased from Sigma-Aldrich or other commercial sources, dried using a Vacuum Atmospheres DRI-SOLV Solvent Purification system, and stored over either 3 or 4 Å molecular sieves. All deuterated solvents were purchased from Cambridge Isotope Laboratories Inc. and were dried over either 3 Å or 4 Å molecular sieves. UCl<sub>4</sub> was prepared following literature procedures.<sup>58</sup> The lithium *tert*-butoxide was prepared through the addition of an equimolar amount of *n*-BuLi to <sup>t</sup>BuOH in hexanes and recrystallized from pentane. All other reagents were obtained from commercial sources and used as received. NMR spectra were recorded on a Varian UNITY INOVA 400 or a Varian UNITY INOVA 500 spectrometer. <sup>1</sup>H and <sup>13</sup>C{<sup>1</sup>H} NMR spectra are referenced to external SiMe<sub>4</sub> using the residual protio solvent peaks as internal standards (<sup>1</sup>H NMR experiments) or the characteristic resonances of the solvent nuclei (<sup>13</sup>C NMR experiments). <sup>7</sup>Li{<sup>1</sup>H} NMR spectra are referenced to external saturated solution of LiCl in deuterium oxide. Elemental analyses were performed by the Micro-Mass Facility at the University of California, Berkeley.

**Cyclic Voltammetry Measurements.** CV experiments were performed using a CH Instruments 600c Potentiostat, and the data were processed using CHI software (version 6.29). All experiments were performed in a glovebox using a 20 mL glass vial as the cell.

(57) Mook, K. H.; Macgregor, S. A.; Heath, G. A.; Derrick, S.; Boeré, R. T. *Dalton Trans.* **1996**, 2067–2076.

(58) Kiplinger, J. L.; Morris, D. E.; Scott, B. L.; Burns, C. J. *Organometallics* **2002**, *21*, 5978–5982.

The working electrode consisted of a platinum disk embedded in glass (2 mm diameter), the counter electrode was a platinum wire, and the reference electrode consisted of AgCl plated on silver wire. Solutions employed during CV studies were typically 3 mM in the uranium complex and 0.1 M in  $[\text{Bu}_4\text{N}][\text{PF}_6]$ . All potentials are reported versus the  $[\text{Cp}_2\text{Fe}]^{0/+}$  couple. For all trials,  $i_{p,a}/i_{p,c} = 1$  for the  $[\text{Cp}_2\text{Fe}]^{0/+}$  couple, whereas  $i_{p,c}$  increased linearly with the square root of the scan rate (i.e.,  $\sqrt{\nu}$ ). Redox couples that exhibited behavior similar to the  $[\text{Cp}_2\text{Fe}]^{0/+}$  couple were thus considered reversible.

**$[\text{Li}(\text{THF})]_2[\text{U}(\text{O}^t\text{Bu})_6]$  (**1**).** To a cold, stirring solution ( $-25^\circ\text{C}$ ) of lithium *tert*-butoxide (0.253 g, 3.16 mmol) in  $\text{Et}_2\text{O}$  (8 mL) was added  $\text{UCl}_4$  (0.200 g, 0.527 mmol) in THF (1.0 mL) dropwise. The resulting solution quickly turned aquamarine, concomitant with codeposition of a light-blue solid and a white solid. This mixture was stirred for 30 min, and the solvent was removed under reduced pressure. The solids were then washed with hexanes ( $3 \times 3$  mL) to remove any soluble side products and residual lithium *tert*-butoxide. The insoluble fraction was then dissolved in  $\text{Et}_2\text{O}$  (15 mL) and filtered through a Celite column (2 cm  $\times$  0.5 cm) supported on glass wool. The volume of the filtrate was reduced in vacuo and solution cooled to  $-25^\circ\text{C}$  for 2 h, resulting in the deposition of light-blue crystals, which were collected and dried under vacuum to give 0.246 g of material. Subsequent concentration and cooling of the supernatant provided a further 0.021 g of turquoise crystals, for a total yield of 61%.  $^1\text{H}$  NMR (500 MHz,  $22^\circ\text{C}$ , THF- $d_8$ ): 1.51 (br s, 54H,  $\text{CCH}_3$ ).  $^7\text{Li}\{^1\text{H}\}$  NMR (194 MHz,  $22^\circ\text{C}$ , THF- $d_8$ ):  $\delta$  2.72 (s).  $^1\text{H}$  NMR (400 MHz,  $22^\circ\text{C}$ ,  $\text{C}_6\text{D}_6$ ):  $\delta$  1.25 (s, 8H,  $\alpha$ -THF protons), 1.31 (br s, 18H,  $\text{CCH}_3$ ), 1.90 (br s, 18H,  $\text{CCH}_3$ ), 2.40 (br s, 18H,  $\text{CCH}_3$ ), 3.16 (s, 8H,  $\beta$ -THF protons).  $^7\text{Li}\{^1\text{H}\}$  NMR (194 MHz,  $22^\circ\text{C}$ ,  $\text{C}_6\text{D}_6$ ):  $\delta$   $-0.91$  (s),  $-1.66$  (s).  $^1\text{H}$  NMR (500 MHz,  $30^\circ\text{C}$ , toluene- $d_8$ ):  $\delta$  1.17 (br s, 18H,  $\text{CCH}_3$ ), 1.35 (s, 8H,  $\alpha$ -THF protons), 1.81 (br s, 18H,  $\text{CCH}_3$ ), 2.33 (br s, 18H,  $\text{CCH}_3$ ), 3.21 (s, 8H,  $\beta$ -THF protons).  $^7\text{Li}\{^1\text{H}\}$  NMR (194 MHz,  $30^\circ\text{C}$ , toluene- $d_8$ ):  $\delta$   $-1.19$  (s),  $-2.14$  (s).  $^1\text{H}$  NMR (500 MHz,  $60^\circ\text{C}$ , toluene- $d_8$ ):  $\delta$  1.43 (s, 8H,  $\alpha$ -THF protons), 1.64 (br s, 54H,  $\text{CCH}_3$ ), 3.34 (s, 8H,  $\beta$ -THF protons).  $^7\text{Li}\{^1\text{H}\}$  NMR (194 MHz,  $60^\circ\text{C}$ , toluene- $d_8$ ):  $\delta$   $-2.06$  (s),  $-3.74$  (s). Anal. Calcd for  $\text{C}_{32}\text{H}_{70}\text{Li}_2\text{O}_8\text{U}$ : C, 46.04; H, 8.47. Found: C, 45.96; H, 8.72.

**$[\text{Li}(\text{THF})][\text{U}_2(\text{O}^t\text{Bu})_9]$  (**2**).** To a solution of lithium *tert*-butoxide (0.190 g, 2.37 mmol) in hexanes (5 mL) with THF (1.0 mL) was added  $\text{UCl}_4$  (0.200 g, 0.527 mmol) while stirring. The solution slowly turned dark green over the course of 5 h, and white precipitate was deposited. The solution was then filtered through a Celite column (2 cm  $\times$  0.5 cm) supported on glass wool. The volume of the filtrate was reduced in vacuo, and the solution was cooled to  $-25^\circ\text{C}$  for 48 h affording green crystals, 0.174 g, 54% yield.  $^1\text{H}$  NMR (500 MHz,  $22^\circ\text{C}$ , THF- $d_8$ ):  $\delta$   $-13.10$  (s, 18H,  $\text{CCH}_3$ ),  $-1.82$  (s, 36H,  $\text{CCH}_3$ ), 1.77 (s, 4H,  $\alpha$ -THF protons), 3.61 (s, 4H,  $\beta$ -THF protons), 12.11 (s, 18H,  $\text{CCH}_3$ ), 22.10 (s, 9H,  $\text{CCH}_3$ ).  $^7\text{Li}\{^1\text{H}\}$  NMR (194 MHz,  $22^\circ\text{C}$ , THF- $d_8$ ):  $\delta$   $-32.28$  (s).  $^1\text{H}$  NMR (500 MHz,  $22^\circ\text{C}$ ,  $\text{C}_6\text{D}_6$ ):  $\delta$   $-6.10$  (br s,  $\text{CCH}_3$ ), 0.96 (br s,  $\text{CCH}_3$ ), 1.80 (s, 4H,  $\alpha$ -THF protons), 2.43 (s, 4H,  $\beta$ -THF protons), 6.10 (br s,  $\text{CCH}_3$ ).  $^7\text{Li}\{^1\text{H}\}$  NMR (194 MHz,  $22^\circ\text{C}$ ,  $\text{C}_6\text{D}_6$ ):  $\delta$   $-18.01$  (s).  $^1\text{H}$  NMR (500 MHz,  $22^\circ\text{C}$ , toluene- $d_8$ ):  $\delta$   $-4.08$  (br s,  $\text{CCH}_3$ ), 1.60 (br s,  $\text{CCH}_3$ ), 1.82 (s, 4H,  $\alpha$ -THF protons), 2.71 (s, 4H,  $\beta$ -THF protons), 4.60 (br s,  $\text{CCH}_3$ ).  $^7\text{Li}\{^1\text{H}\}$  NMR (194 MHz,  $22^\circ\text{C}$ , toluene- $d_8$ ):  $\delta$   $-17.87$  (s).  $^1\text{H}$  NMR (500 MHz,  $-15^\circ\text{C}$ , toluene- $d_8$ ):  $\delta$   $-11.57$  (s, 18H,  $\text{CCH}_3$ ),  $-1.05$  (s, 36H,  $\text{CCH}_3$ ), 11.15 (s, 18H,  $\text{CCH}_3$ ), 19.66 (s, 9H,  $\text{CCH}_3$ ).  $^7\text{Li}\{^1\text{H}\}$  NMR (194 MHz,  $-15^\circ\text{C}$ , toluene- $d_8$ ):  $\delta$   $-33.48$ .  $^1\text{H}$  NMR (500 MHz,  $70^\circ\text{C}$ , toluene- $d_8$ ):  $\delta$  1.52 (br s, 81H,  $\text{CCH}_3$ ), 2.07 (s, 4H,  $\alpha$ -THF protons), 3.27 (s, 4H,  $\beta$ -THF protons).  $^7\text{Li}\{^1\text{H}\}$  NMR (194 MHz,  $70^\circ\text{C}$ , toluene-

$d_8$ ):  $\delta$   $-0.50$  (s). Anal. Calcd for  $\text{C}_{40}\text{H}_{89}\text{LiO}_{10}\text{U}_2$ : C, 39.60; H, 7.39. Found: C, 39.48; H, 7.37.

**$[\text{Li}(\text{Et}_2\text{O})][\text{U}(\text{O}^t\text{Bu})_6]$  (**3**· $\text{Et}_2\text{O}$ ).** To a stirring solution of **1** (0.013 g, 0.016 mmol) in toluene (3.0 mL) was added  $\text{I}_2$  (0.002 mg, 0.007 mmol). The reaction mixture immediately turned colorless. The solution was stirred for 4 h while a white precipitate slowly deposited. The mixture was then filtered through a Celite column (2 cm  $\times$  0.5 cm) supported on glass wool, and the volatiles were removed in vacuo to give a colorless solid. The solid was dissolved in  $\text{Et}_2\text{O}$  (1.0 mL) yielding a pale-yellow solution, and clear crystals were recovered by evaporation of the solvent at  $-25^\circ\text{C}$  over 48 h, 0.003 g, 25% yield.  $^1\text{H}$  NMR (500 MHz,  $22^\circ\text{C}$ ,  $\text{C}_6\text{D}_6$ ):  $\delta$  0.93 (s, 6H,  $\beta$ - $\text{Et}_2\text{O}$  protons), 2.00 (s, 54H,  $\text{CCH}_3$ ), 2.97 (s, 4H,  $\alpha$ - $\text{Et}_2\text{O}$  protons).  $^{13}\text{C}\{^1\text{H}\}$  NMR (125 MHz,  $22^\circ\text{C}$ ,  $\text{C}_6\text{D}_6$ ):  $\delta$  14.95 ( $\beta$ - $\text{Et}_2\text{O}$  carbons), 43.69 ( $\text{CCH}_3$ ), 66.16 ( $\alpha$ - $\text{Et}_2\text{O}$  carbons), 101.83 ( $\text{CCH}_3$ ).  $^7\text{Li}\{^1\text{H}\}$  NMR (194 MHz,  $22^\circ\text{C}$ ,  $\text{C}_6\text{D}_6$ ):  $\delta$  6.75 (s).

**$[\text{Li}(\text{THF})][\text{U}(\text{O}^t\text{Bu})_6]$  (**3**·THF).** To a stirring solution of  $\text{U}(\text{O}^t\text{Bu})_6$  (0.010 g, 0.015 mmol) in THF (3.0 mL) was added **1** (0.012 g, 0.015 mmol) at room temperature. The solution immediately turned colorless. The solvent was removed in vacuo to give a white powder, 0.021 g, 98% yield.  $^1\text{H}$  NMR (500 MHz,  $22^\circ\text{C}$ ,  $\text{C}_6\text{D}_6$ ):  $\delta$  1.17 (s, 4H,  $\alpha$ -THF protons), 2.02 (s, 54H,  $\text{CCH}_3$ ), 3.30 (s, 4H,  $\beta$ -THF protons).  $^7\text{Li}\{^1\text{H}\}$  NMR (194 MHz,  $22^\circ\text{C}$ ,  $\text{C}_6\text{D}_6$ ):  $\delta$  4.21 (s). Anal. Calcd for  $\text{C}_{28}\text{H}_{62}\text{LiO}_7\text{U}$ : C, 44.50; H, 8.27. Found: C, 44.54; H, 8.16.

**$\text{U}(\text{O}^t\text{Bu})_6$  (**4**).** To a stirring suspension of **1** (0.100 g, 0.120 mmol) in pentane (5.0 mL) was added dropwise a solution of  $\text{I}_2$  (0.030 g, 0.120 mmol) in pentane (3.0 mL) at room temperature. After 4 h, the dark-red solution was filtered through a Celite column (2 cm  $\times$  0.5 cm) supported on glass wool, and the volatiles were removed in vacuo to give 0.078 g of red powder. The red solid was redissolved in pentane (3.0 mL), and red crystals were recovered by slow evaporation of the solvent at  $-25^\circ\text{C}$  over 1 week, 0.050 g, 61% yield.  $^1\text{H}$  NMR (500 MHz,  $22^\circ\text{C}$ ,  $\text{C}_6\text{D}_6$ ):  $\delta$  1.67 (s, 54H,  $\text{CCH}_3$ ).  $^{13}\text{C}\{^1\text{H}\}$  NMR (125 MHz,  $22^\circ\text{C}$ ,  $\text{C}_6\text{D}_6$ ):  $\delta$  36.13 ( $\text{CCH}_3$ ), 92.25 ( $\text{CCH}_3$ ). This complex has been previously prepared.<sup>15,16</sup>

**X-ray Crystallography.** Data for **1**, **2**· $\text{C}_5\text{H}_{12}$ , **3**· $\text{Et}_2\text{O}$ , and **4** were collected on a Bruker 3-axis platform diffractometer equipped with a SMART-1000 CCD detector using a graphite monochromator with a Mo  $\text{K}\alpha$  X-ray source ( $\alpha = 0.71073 \text{ \AA}$ ). The crystals were mounted on a glass fiber under Paratone-N oil, and all data were collected at 150(2) K using an Oxford nitrogen gas cryostream system. A hemisphere of data was collected using  $\omega$  scans with 10–15 s frame exposures and  $0.3^\circ$  frame widths. Data collection and cell parameter determination was conducted using the SMART program.<sup>59</sup> Integration of the data frames and final cell parameter refinement were performed using SAINT software.<sup>60</sup> Absorption correction of the data was carried out empirically based on reflection  $\Psi$ -scans. Subsequent calculations were carried out using SHELX-TL.<sup>61</sup> Structure determination was done using direct or Patterson methods and difference Fourier techniques. All hydrogen atom positions were idealized and rode on the atom of attachment with exceptions noted in subsequent paragraphs. Structure solution, refinement, graphics, and creation of publication materials were performed using SHELXTL.<sup>61</sup>

**1**, **2**· $\text{C}_5\text{H}_{12}$ , and **4** possessed disorder about the quaternary carbons of some *tert*-butoxide groups. The ligand disorder was

(59) SMART Software Users Guide, Version 5.1; Bruker Analytical X-ray Systems, Inc.: Madison, WI, 1999.

(60) SAINT Software Users Guide, Version 5.1; Bruker Analytical X-ray Systems, Inc.: Madison, WI, 1999.

(61) Sheldrick, G. M. SHELXTL, 6.12; Bruker Analytical X-Ray Systems, Inc.: Madison, WI, 2001.

### Three Homoleptic Alkoxides of Uranium

addressed by assigning the groups in two positions, and occupancy was determined through data refinement. Restraints were applied to the disordered *tert*-butoxide groups by fixing the C–C bond lengths between the quaternary and methyl carbons to 1.50(1) Å, the C–O bond lengths to 1.40(1) Å, and constraining the involved carbon atom to have ideal tetrahedral geometry. Idealized hydrogens were not assigned to the disordered carbons. For **3**•Et<sub>2</sub>O, which crystallizes in the noncentrosymmetric space group of *Imm2*, the Flack parameter was 0.2122 and the structure was refined as a racemic twin with a ratio of components of 76:24. A summary of

relevant crystallographic data for **1**, **2**•C<sub>5</sub>H<sub>12</sub>, **3**•Et<sub>2</sub>O, and **4** is presented in Table 1.

**Acknowledgment.** We thank the University of California, Santa Barbara, for financial support of this work.

**Supporting Information Available:** X-ray crystallographic details (CIF files) of **1**, **2**•C<sub>5</sub>H<sub>12</sub>, **3**•Et<sub>2</sub>O, and **4**; tabulated cyclic voltammetry data for **4**; NMR spectra of **1** and **2**. This material is available free of charge via the Internet at <http://pubs.acs.org>.

IC800067K